



# TOWARDS A CONCURRENT NUMERICAL PREDICTION OF HEAT TRANSFER PHENOMENA PRESENT IN IVR-ERVC DURING A SEVERE ACCIDENT IN APR1400 REACTORS

Muritala A. Amidu<sup>1,2\*</sup>, Yacine Addad<sup>1,2</sup>, Imran Afgan<sup>1,3</sup>

<sup>1</sup>College of Engineering, Khalifa University, P.O. Box 127788, UAE

<sup>2</sup>Emirates Nuclear Technology Centre, Khalifa University, P.O. Box 127788, UAE

<sup>3</sup>Department of MACE, College of Engineering, University of Manchester, M13 9PL, UK

## ABSTRACT

In an effort to develop a holistic CFD method that is capable of simulating the complicated phenomena in IVR-ERVC severe accident mitigation strategy simultaneously, physical models are developed to capture some important physics such as melting, solidification, natural convection and slug flow boiling in IVR-ERVC mitigation system and these models are validated against experimental separate effect test data. Furthermore, a decoupled simulation of IVR is performed for APR1400 reactors to investigate potential failure of the reactor pressure vessel at the location of in-core instrumentation and location of the focusing effect. To this end, a two-layer IVR configuration is assessed and the integrity of the RPV is found not to be compromised under external reactor vessel cooling. Focusing on the in-core instrumentation location, severe ablations of the cladding and the weld materials are observed at a heat load of about ~ 1800 K which is expected to lead to the ejection of the penetration tubes if the force holding the penetration tube in place is lower than the force exerted by the system pressure. However, in the case of a boiling crisis, the temperature of the ex-vessel wall is expected to rise quickly and this is simulated by increasing the ex-vessel wall temperature. The RPV is found to fail near the beltline due to a phenomenon known as focusing effect when the ex-vessel wall temperature rises above 1200 K. Thus, a coupled IVR-ERVC simulation is required to provide more reliable evaluation of the performance of the mitigation strategy and we intend to accomplish this in the future.

## 1. INTRODUCTION

The In-Vessel Retention (IVR) through External Reactor Vessel Cooling (ERVC) is a severe accident management strategy for APR1400 and other high-power nuclear reactors. With this strategy, the reactor cavity is flooded before the relocation of molten corium to the lower plenum of the reactor pressure vessel. The decay heat of the molten corium when it reaches the lower plenum is transferred to the external surface of the reactor vessel through convection in the molten corium and conduction through the vessel walls. This heat is eventually removed via convection heat transfer of water existing between the Reactor Pressure Vessel (RPV) and the cavity. The heat transfer phenomena such as natural convection of molten corium, solidification of corium, melting of the RPV, conduction in the RPV, and nucleate boiling at the ex-vessel surface that are present in IVR-ERVC are interdependent and their location of occurrence are shown in Figure 1. The ultimate goal is to provide a CFD tool that can concurrently predict all these phenomena. To achieve this, the problem is first divided into segments viz: IVR and ERVC (shown in Figure 1) to allow separate effect tests for validations of various physical models. It is important to clarify that the prediction of the coupled IVR and ERVC segments is not included in this article. Thus, this paper presents recently developed physical models for capturing the physics of these heat transfer phenomena in CFD code at Khalifa University of Science and Technology. With this CFD code, improved prediction of the dominant phenomena in the course of accident progression would aid the development of severe accident management guidelines (SAMG) not only for the APR1400 but also the plants currently in the design phase.

\*Corresponding Author: [amidu.alade@ku.ac.ae](mailto:amidu.alade@ku.ac.ae)

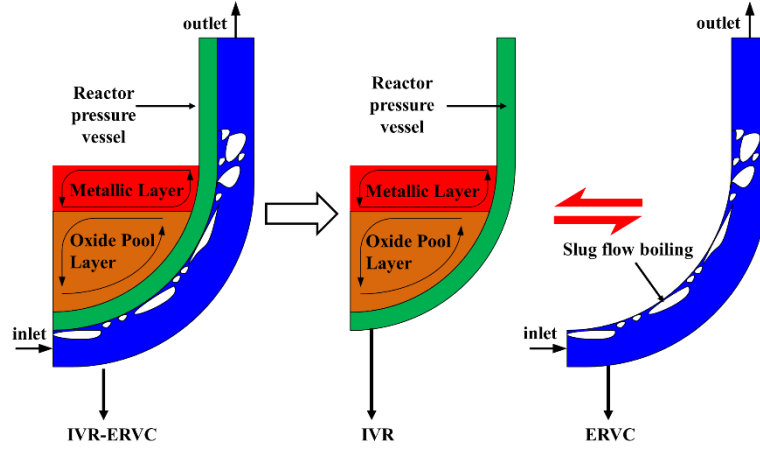


Figure 1 Schematic diagram of heat transfer phenomena present in IVR-ERVC of an APR1400 reactor

## 2. PHENOMENOLOGICAL PREDICTION OF THE IVR-ERVC

Considering the decoupled IVR-ERVC (shown in Fig. 1), The dominant heat transfer mechanism in IVR are natural convection of the core melt, solidification of the core melt, melting and heat conduction in the RPV while the dominant heat transfer mechanisms in ERVC are slug flow boiling and critical heat flux condition. As of now, the heat transfer mechanisms in IVR are coupled and treated separately from those of the ERVC so as to allow separate effect tests to validate the various models used to capture the physics of these phenomena prior to the deployment of the models for the prediction of integrated IVR-ERVC. Numerical models that better capture the physics of these heat transfer mechanisms are, therefore, essential towards a reliable performance evaluation of the IVR-ERVC strategy.

### 2.1 Models for phenomena in in-vessel retention (IVR) and validation

The key phenomena present in IVR are natural convection of the corium melt, solidification of the corium melt and melting of the reactor pressure vessel. The CFD model used to capture these phenomena is based on the enthalpy-porosity method [1, 2] which involves the following governing equations of mass, momentum and energy.

Continuity equation:

$$\nabla \cdot (u) = 0 \quad (1)$$

Momentum equation:

$$\frac{\partial(\rho u)}{\partial t} + \nabla \cdot (\rho u u) = \nabla \cdot (\eta_T \nabla u) - \frac{\partial p}{\partial x} + S_m + S_b \quad (2)$$

Energy equation:

$$\frac{\partial(\rho c T)}{\partial t} + \nabla \cdot (\rho u c T) = \nabla \cdot (\lambda \nabla T) - \nabla \cdot q_t + S_h + q_v \quad (3)$$

where the porosity source term ( $S_m$ ) in the momentum equations, buoyancy source term ( $S_b$ ) in the momentum equation and the enthalpy source term ( $S_h$ ) in the energy equation are defined as shown in the following equation (Eq. (4)).

$$S_m = -u C \frac{(1-\alpha)^2}{\alpha^{3+b}}; S_b = \rho g \cdot [1 - \beta \cdot (T - T_s)]; S_h = -\rho L \frac{4 \cdot \exp\left(\left(\frac{4(T-T_m)}{T_l-T_s}\right)^2\right)}{(T_l-T_s)\sqrt{\pi}} \cdot \left(\frac{\partial T}{\partial t} + u \nabla T\right) \quad (4)$$

where  $c$ ,  $\rho$ ,  $\lambda$ , and  $u$  represent the specific heat capacity, density, thermal conductivity, and the velocity vector of the phase changing material, respectively. Also,  $q_t$  is the turbulent heat flux,  $\alpha$  is the liquid fraction,  $p$  is the system pressure,  $\eta_T$  is the total dynamic viscosity which is the sum of molecular and turbulent viscosity. To capture the solidification and melting of corium melt and the reactor pressure vessel as their temperature goes below or above their melting points, an error function is used to transform the liquid fraction between  $\alpha = 1$  and  $\alpha = 0$  for melting ( $\alpha = 0 \rightarrow 1$ ) and solidification ( $\alpha = 1 \rightarrow 0$ ) processes as can be seen in the definition of the  $S_h$  in Eq. (4) where  $T_l$  is the liquidus (liquid phase temperature),  $T_s$  is the solidus (solid-phase temperature), and  $T_m$  is the melting temperature defined as the arithmetic average of the solidus and liquidus. Also, the  $C$  constant in the porosity source term ( $S_m$ ) in Eq. (4) has a recommended value of  $1.6 \times 10^3$  and  $b$  is a small numerical constant with a value of about 0.001 used to avoid division by zero in the equation. The buoyancy source term ( $S_b$ ) is derived from the Boussinesq approximation.

The melting/solidification model is validated using the experimental geometry and conditions of Gau and Viskanta [3] for melting of Gallium in a rectangular cavity. The melt front of the Gallium at simulation time of 13 minutes is shown Figure 2(a) which shows that the melting process progresses faster at the upper part of the cavity. The temporal positions of the liquid/solid boundary measured by Gau and Viskanta [3] are compared with the numerical prediction in the present study as shown in Figure 2(b). The comparison shows that the modified enthalpy-porosity method can simulate the melting process with a fair agreement in the prediction of the melt front.

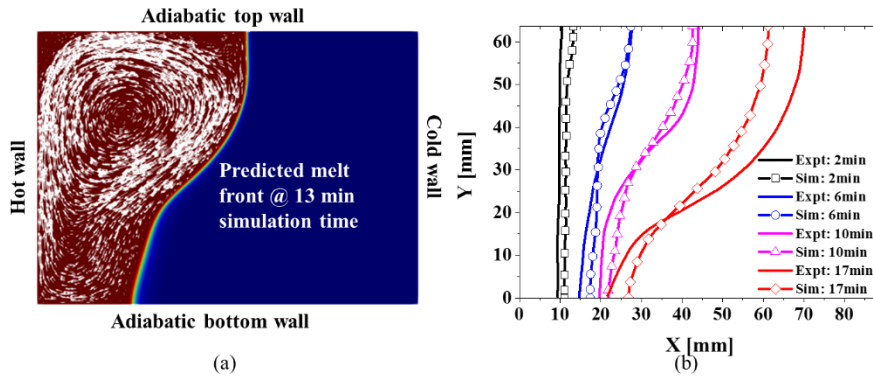


**Figure 2:** Validation of the melting/solidification model: (a) Liquid fraction distribution of Gallium at simulation time of 13 minutes, (b) Comparison of the predicted melt front with experimental data [1].

Furthermore, BALI experimental setup [4] is used in this study for the verification and validation of the turbulence models for the prediction of natural convection of the corium melt in IVR-ERVC configuration. The qualitative simulation result for  $k - \omega$  SST turbulence model is presented in Figure 3(a) which shows stratification of the temperature field with the liquid having higher temperature in the top region where there appears to be no disturbance in the flow.

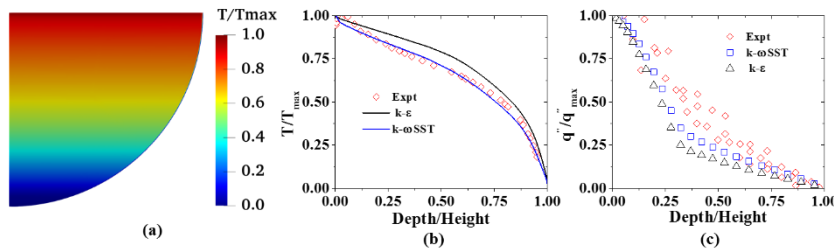


**Figure 3:** Validation against BALI experiment: (a) Qualitative temperature distribution, (b) Temperature profile along the vertical wall, (c) Heat flux profile along the curved wall [1].

For quantitative simulation results, Figure 3(b) and Figure 3(c) show a dimensionless temperature profile along the vertical wall and dimensionless heat flux profile along the curved surface. The results show that  $k - \omega$  SST provides better performance than  $k - \varepsilon$  in predicting the temperature and the heat flux profiles. In light of this, it can be said that  $k - \omega$  SST turbulence model can reproduce, more accurately, the general characteristics of the convective heat transfer in the BALI experiment and it is, therefore, employed for the prediction of natural convection heat transfer present in the metallic and ceramic pool layers as discussed later in this article.

## 2.2 Model for Phenomena in external reactor vessel cooling (ERVC) and validation

As stated earlier, two key phenomena that are present in ERVC are the slug flow boiling and occurrence of critical heat flux condition. In terms of modelling, only slug flow boiling is covered in this section while critical heat flux phenomena is a subject of future consideration. The nucleate boiling on the external surface of the RPV (ERVC) is characterized by the presence of vapor slugs (shown in Figure 2(a)) due to the downward-facing orientation of the heated surface. Hence it is called slug flow boiling. The two-phase natural convection flow in the cavity involves the simultaneous occurrence of bubble flow regimes (dispersed gas interface structure) and slug /churn-turbulent regimes (large bubble interface structures) illustrated in Figure 2(b). To capture these flow characteristics, a hybrid volume of fluid – Eulerian model [1] is implemented within the solution framework of OpenFOAM CFD. However, the existing wall boiling model (based on small spherical bubbles) which is a combination of convection ( $q_c''$ ), evaporation ( $q_e''$ ), and quenching ( $q_q''$ ) heat fluxes (see Eq. (1)) has to be enhanced to account for the heat transfer mode of slug bubbles ( $q_\delta''$ ) on the wall (see Eq. (2)) as was done in previous studies [5, 6, 7, 8]. Where,  $H(\alpha_s)$  is the blending function (linear) between the small bubble regime and the large bubble (slug) regime. The existing models and the empirical correlation used by the MELCOR code (the default code used by the nuclear industry for severe accidents simulations) either over or under predict the wall superheat. In contrast, the presented extended model not only better captures the flow physics, but also provides more precise heat transfer characteristics of flow boiling involving sliding slug bubbles as shown in Figures 2(c).

$$q_{NB}'' = q_c'' + q_e'' + q_q'' \quad (1)$$

$$q_w'' = [1 - H(\alpha_s)]q_{NB}'' + H(\alpha_s)q_\delta'' \quad (2)$$

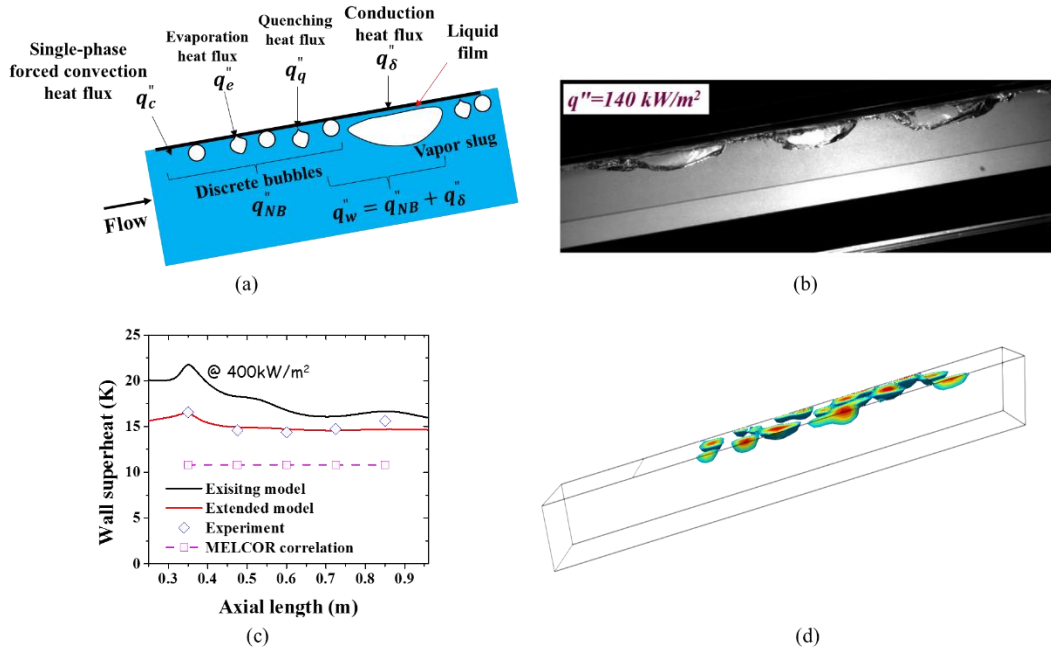


**Figure 4:** Prediction of ex-vessel nucleate boiling: (a) Experimental observation of vapour slugs; (b) Extension of wall boiling model to cover vapour slug heat transfer; (c) Comparison of the predicted wall superheat with experimental data; (d) Iso-surface of the vapor slugs at simulation time of 2.5 s [6].

### 3. INVESTIGATION OF THE POTENTIAL RPV FAILURE IN IVR-ERVC

Using the model described above, two failure modes of the reactor pressure vessel under the thermal load of the molten corium are investigated. The first failure mode is potential failure of the RPV at the location of in-core instrumentation (ICI) due to the melting of the welding materials which is the most vulnerable point of attack by the molten corium during a severe accident. The second failure mode is the focusing effect of the metallic layer which could lead to the rupture of the RPV due to a very high heat flux imposed on the RPV by the metallic layer. Using the experimental test sample of An et al. [9] which is shown in Fig. 5(a), a fairly good prediction of the temperature profile of the welding material is obtained while the temperature profiles in the penetration tube and reactor vessel are over predicted as can be seen in Fig. 5(b). This could result from the uniform initial conditions used for the constituent materials. Moreover, with the imposition of a constant temperature of  $\sim 400\text{K}$  at the bottom surface in place of the adiabatic condition earlier imposed, the liquid fractions of the constituent materials show no significant reduction of the ablation rate as shown in Fig. 5(c). This implies that the welding materials would always fail under the thermal attack by molten corium expulsion of the molten corium at this location depends on whether the system pressure can produce a driving force that could overcome the binding force resulting from the differential thermal expansion of the penetration tube (ICI).

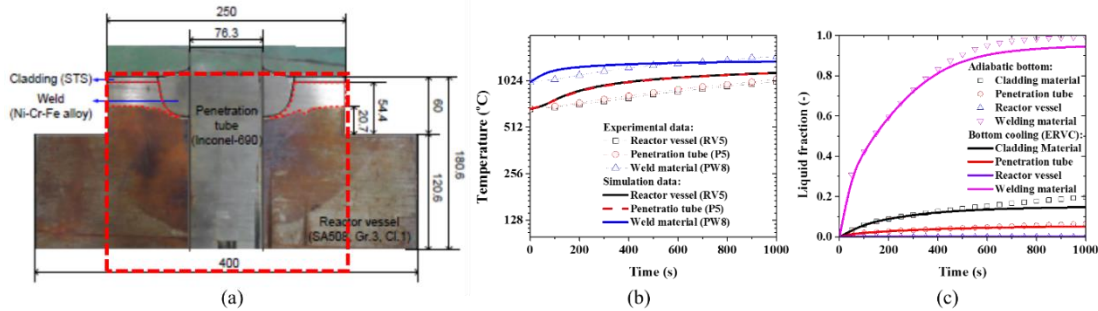


**Figure 5:** (a) Experimental test specimen used for simulation; (b) Comparison of transient temperature profile of simulation with experiment; (c) Ablation of the reactor pressure vessel at the location of ICI [1].

For the investigation of the focusing effect, a two-layer IVR configuration (shown in Fig. 6(a)) consisting of three distinct regions (metallic layer, ceramic pool layer, and reactor pressure vessel) is considered in this study. Note that the ERVC is not coupled with the IVR in this study, instead, a constant temperature boundary condition is imposed at the external surface of the reactor pressure vessel. The natural convections of the molten corium in both the metallic layer and the oxide pool layer shown in Fig. 6(b) are captured using  $k - \omega$  SST turbulence model which has been earlier validated as discussed in the previous section. Provided normal nucleate boiling (represented by wall temperature of 400 K) is sustained at the external wall of the RPV, the integrity of the reactor pressure is predicted to be maintained as can be seen in Fig. 6(c). However, in case of boiling crisis (critical heat flux condition), jump in temperature at the ex-vessel wall could cause rupture of the vessel wall at the location of the focusing effect as demonstrated in Fig. 6(c) when the ex-vessel wall temperature boundary condition is increased up to 1400 K. Therefore, in addition to the ex-vessel cooling, in-vessel flooding has been suggested to arrest the transient focusing effect because it gives much better evacuation of heat from the top surface of the metallic layer than the radiative heat transfer. Consequently, this in-vessel flooding could reduce the risk of vessel failure due to the focusing effect.

### 4. CONCLUSION

This paper presents the development and validation of models for some dominant heat transfer phenomena such as melting/solidification, slug flow boiling and natural convection, occurring in IVR-ERVC system of APR1400 reactor during a severe accident scenario. These models are integrated in CFD code to investigate two potential failure modes of the reactor pressure vessel under thermal attack

from the molten corium. First, the welding material is found to completely ablate and fail at the location of the in-core instrumentation (penetration tube). This could result in the ejection of the penetration tube thereby causing corium leakage provided that the system pressure is high enough to overcome the binding force between the penetration tube and the reactor pressure vessel. Second, the reactor pressure vessel integrity is intact when the normal nucleate boiling occurs at the external surface of the RPV. Whereas, at the occurrence of boiling crisis (attainment of critical heat flux condition), the reactor pressure vessel is found to fail by rupture at the location of the focussing effect. In the future, a complete simultaneous simulation of the IVR-ERVC would be performed in lieu of imposition of constant temperature boundary condition at the reactor pressure vessel external surface to represent the ERVC as done in this article. This could also be extended to involving molten corium-concrete interaction [10].

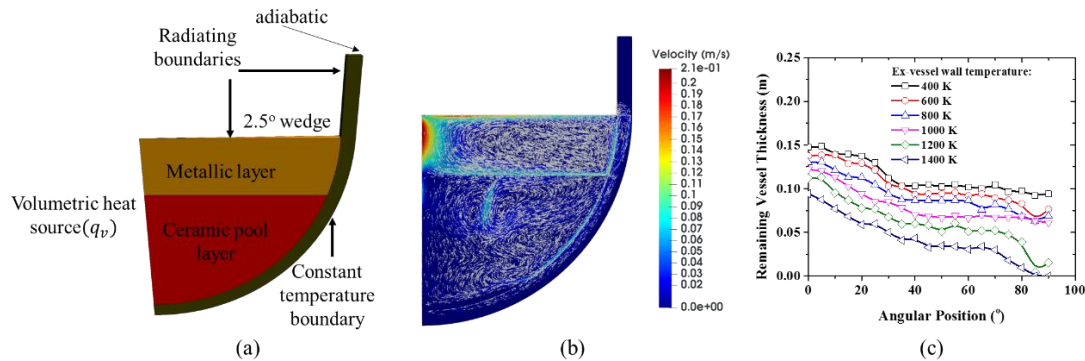


**Figure 6:** Concurrent prediction of the IVR phenomena: (a) A two-layer configuration of IVR showing the boundary conditions; (b) Velocity contour of the liquid regions in the IVR; (c) Effect of ex-vessel wall temperature boundary condition on the remaining vessel thickness [1].

## ACKNOWLEDGEMENTS

The authors would like to thank KU and ENTC for the financial and computational support.

## REFERENCES

- [1] M.A. Amidu, Y. Addad, J.I. Lee, D.H. Kam, Y.H. Jeong. Investigation of the pressure vessel lower head potential failure under IVR-ERVC condition during a severe accident scenario in APR1400 reactors, *Nuclear Engineering and Design*, 134(2021), 111107.
- [2] M.A. Amidu, and Y. Addad, Numerical Prediction of the Reactor Pressure Vessel Melting under IVR-ERVC conditions, International Topical Meeting on Advances in Thermal Hydraulics (2020), France.
- [3] C. Gau and R. Viskanta. Melting and Solidification of a pure metal on a vertical wall, *Journal of Heat Transfer*, 35(1986), 174-181.
- [4] J.M. Bonnet and J.M. Seiler. Thermal hydraulic phenomena in corium pools: the BALI experiment, *In Proceedings of the 7<sup>th</sup> International Conference on Nuclear Engineering*, ICONE-7057(1999), Japan.
- [5] M.A. Amidu, Y. Addad, and M.K. Riahi. A hybrid multiphase flow model for the prediction of both low and high void fraction nucleate boiling regimes, *Applied Thermal Engineering*, Vol. 178 (2020), 115625
- [6] M.A. Amidu, and Y. Addad. An enhanced model for the prediction of slug flow boiling heat transfer on a downward-facing heated wall, *Annals of Nuclear Energy*, 145 (2020), 10596
- [7] M.A. Amidu, and Y. Addad. Bubble-induced enhancement of single-phase liquid forced convection heat transfer during subcooled nucleate flow boiling, *Annals of Nuclear Energy*, 134 (2019), 60-66.
- [8] M.A. Amidu, and H. Kim. Modeling and simulation of flow boiling on a downward facing heating surface in the presence of vapor slug, *Nuclear Engineering and Design*, 351 (2019), 175-188
- [9] S.M. An, J. Jung, K.S. Ha, and H.Y. Kim. Experimental investigation on APR1400 In-Core Instrumentation penetration failure during a severe accident, *Proceeding of ICAPP*, Paper 15446 (2015), May 03 – 06, Nice, France.
- [10] M.A. Amidu, and Y. Addad. The influence of the water ingress and melt eruption model on the MELCOR code prediction of molten-concrete interaction in APR1400 reactor cavity, *Nuclear Engineering and Technology*, (2021), <https://doi.org/10.1016/j.net.2021.09.036>.